Songklanakarin J. Sci. Technol.
44 (2), 316-322, Mar. - Apr. 2022

http://www.sjst.psu.ac.th

Original Article

Performance analysis of AA3103 and AA6063 dissimilar weld joints by friction stir welding

T. Kannan[1], B. Arulmurugan[1], L. Feroz ali[2], and L. Rajeshkumar[1]

[1] *Department of Mechanical Engineering, KPR Institute of Engineering and Technology, Coimbatore, Tamilnadu, 641407 India*

[2] *Department of Mechatronics Engineering, Sri Krishna of Engineering and Technology, Coimbatore, Tamilnadu, 641008 India*

Received: 30 April 2019; Revised: 18 July 2021; Accepted: 25 August 2021

Abstract

Frictional heating system and permanent distortion under melting heat are mechanisms behind Friction stir welding (FSW) of materials. The main aim of this investigation was to examine the influences of mechanical characteristics of friction stir welded dissimilar aluminium alloys (AA3103 & AA6063) on various joining parameters and to perform ANSYS analysis to assess the temperature distribution in the welded area. Properties like hardness and tensile strength were investigated to assess the mechanical performance of the welded alloys by considering parameters like welding speed, tool rotation speed, and the applied axial load. It could be seen from the results that a rotational speed of 1300 rpm, welding speed of 30 mm/min and an axial load of 9 kN provided maximum tensile strength and hardness to the FSW specimen. Temperature distribution during the welding was visualized using ANSYS.

Keywords: aluminium alloys, friction stir welding, ANSYS, hardness, tensile strength

1. Introduction

Aluminium 3 series alloys have good strength and machinability and so they are widely used in automotive industry, aerospace industry, in construction of machines, appliances, and structures, as cooking utensils, and in architectural applications for making critical structure materials, contributing 90% of all shaped castings produced (Kumar *et al*., 2020a; Rajkumar *et al*., 2021a, 2021b; Raj kumar, Arulmurugan, Manikandan, Karthick & Kaviprasath, 2017). Aluminium alloys have good strength to weight ratio and formability, which encourage the use aluminium in many industries (Rajeshkumar 2018; Rajkumar, Arulmurugan & Muthuraman, 2018; Saravanakumar, Bhuvaneswari & Gokul, 2020a). Fusion welding is the only possible way to weld the 2xxx series Al alloys, but hot cracking, alloy segregation, partially melted zone, and porosity are some of the major drawbacks that must be addressed (Bhuvaneswari *et al*., 2021; Dietrich, Nickel & Krause, 2011; Ganesan *et al*., 2021). Also the pulse generation results have given weld properties of aluminium alloy that were inconsistent (Arulmurugan *et al*., 2021a, 2021b). A world-first process developed by G2 Alloy, called Friction Stir Welding process (FSW), has proven capable of welding dense materials, including aluminium and magnesium alloys in a fast and effective manner. When all the effective parameter combinations were tested in FSW, an alloy covering in two minutes can be especially well welded between two parts (two distinct discontinuous processes) (Anbuchezhian, Devarajan, Priya & Rajeshkumar, 2020; Arulmurugan *et al*., 2020, 2021c; Mishra & Ma, 2005; Nandan, DebRoy & Bhadeshia, 2008; Scialpi, De Filippis & Cavaliere, 2007).

Many studies have performed experiments to research the effects of high-strength and super endurance Al-Zn-Mg-Cu alloys on welding conditions, assessing the morphology and mechanical characteristics of joints

*Corresponding author
Email address: kannantsai@gmail.com

(Genevois, Deschamps, Denquin & Doisneau-Cottignies, 2005; Rajeshkumar *et al*., 2020a; Rajeshkumara & Balajia 2020; Upadhyay & Reynolds, 2010; Xu, Liu, Luan & Dong, 2009; Zhang, Su, Chen & Nie, 2015). The heating of the material caused the heat affected zone (HAZ) to be fundamentally changed and harmed by a temperature rise (Mofid, Abdollah-Zadeh & Ghaini, 2012; Rajeshkumar *et al*., 2020b; Rui-Dong *et al*., 2011;). Few authors have experimented on AA2198-T6 aluminium - lithium alloy joints and evaluated the effects of process parameters on the fatigue properties of FSW components. Investigations have shown that there is also a change in failure mode from brittle fracture to ductile (Amirthagadeswaran, 2019; John *et al*., 2019; Mclean, Powell, Brown & Linton, 2003; Mao *et al*., 2015; Singh, Singh & Singh, 2011; Zettler, Da Silva, Rodrigues, Blanco & dos Santos, 2006). Experiments found the 6082-T651 Aluminium alloy being affected by the FSW parameters in its mechanical characteristics. From this analysis it was stated that the weld quality depends on the welding speed and this plays a major role in defining the mechanical characteristics, including the 85% higher strength than that of the base metal (Arulmurugan & Manikandan, 2018; Manikandan *et al*., 2017; Rajeshkumar & Amirtha gadeswaran, 2019; Saravanakumar, Rajeshkumar, Balaji & Karunan, 2020b; Saravanakumar, Sivalingam & Rajeshkumar, 2018a). It was clear that plenty of studies were assessing the grain size properties and elongation characteristics for various grades of alloys of aluminium with individual friction stir welding parameters (Arulmurugan *et al*., 2019; Manikandan *et al*., 2016; Ramesh, Marimuthu, Karuppuswamy & Rajesh kumar, 2021; Saravanakumar, Saravanakumar, Sivalingam & Bhuvaneswari, 2018b;).

Very few works are available that have determined the mechanical characteristics of dissimilar weld joints when welded through FSW. In view of all the above facts, the current study deals with the evaluation of tensile strength and hardness for dissimilar aluminium alloys AA6063 and AA3103 welded through FSW. The manipulated process parameters were revolving speed, welding speed, and applied load, with three levels for each. Temperature distribution during the FSW was also assessed by using ANSYS.

2. Materials and Methods

2.1 Aluminum alloys AA6063 and AA3103

Aluminium alloy AA6063 is a medium strength alloy, with offline surface finishing to improve corrosion resistance, and is well-suited for joining processes. Anodizing is commonly done. Aluminium alloy AA3103 is used for welded tanks, tubes for transporting petrol and oil, radiators, and other machinery. Due to its high machinability, it can be fabricated in multilayers, which aids them in begetting higher fatigue resistance particularly during cyclic loading. Table 1 shows the chemical compositions of both these aluminium alloys.

Table 1. Chemical compositions of AA6063 and AA3103

S.No	Alloying element	AA6063 composition (%)	AA3103 Composition (%)
1	Chromium	0.1	0.1
2	Copper	0.1	0.1
3	Iron	0.35	0.7
4	Magnesium	0.45–0.9	0.3
5	Manganese	0.1	0.9–1.5
6	Silicon	0.2–0.6	0.2
7	Aluminium	Remaining	Remaining

2.2 FSW experimental setup

Friction stir welding was conducted on a friction stir welding machine. For the current work, a material of dimensions 100 × 50 × 6 mm and a FSW tool of dimensions 5.8 mm length, 20 mm diameter shoulder and 6 mm pin diameter was taken. After trial welding, actual process parameters were set in the FSW machine. With the help of a special fixture, a pair of work pieces was clamped tightly on the table of a milling machine. A rotating non-consumable tool pin plunges into the outermost surfaces until its shoulders touch the surface of the work material. Then a heating cycle was commenced and the tray containing the plates to be welded was pushed at a gradual pace along the direction of heat supplied. When the joint was raised, the applied force acted perpendicular to the joint (Singh *et al*., 2011; Xu *et al*., 2009; Zhang *et al*., 2015). Test heat flux at the free tools system had to be controlled. If the tool projection never reached the angled side of the retained tool body, the actual tool was extracted. Rotational pressure with uniform heat was created when using the process and the fracture energy applied on the specimen was directly correlated with the elbow swing along with the insert and the rate of mixing of the metallic alloys around the friction weld pin, which in turn creates a proper weld. Figure 1 is a schematic of the FSW experimental setup along with the process parameters taken for analysis. Table 2 shows the experimental setup components and their dimensions.

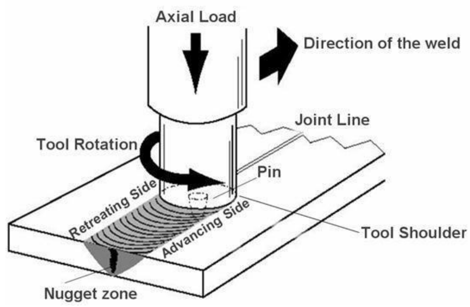

Figure 1. FSW experimental setup

Table 2. FSW tool and work piece dimensions

S.No	Tool and work piece	Dimension (mm)
1	Width of plate 1	100
2	Width of plate 2	5
3	Thickness Plate 1 & 2	6
4	Length of plates	100
5	Shoulder diameter	22
6	Shoulder height	20
7	Pin Diameter	6
8	Pin height	5.7

2.3 Mechanical properties of the weld joints

A Universal Testing Machine was used to determine the tensile strengths of the specimens per the standard ASTM E08. Figure 2 shows a photograph of tensile specimens cut from the welded plate.

Using the Vickers micro-hardness test, the hardness of the welded specimen was determined. Vickers hardness test is done with the same indenter for a range of hardnesses, giving continuous hardness values (typically HV100 to HV500). Different welding speeds and rotational speeds were applied in nine welded specimens. Samples for the micro-hardness test were prepared per ASTM E384 standard, and the hardness of the welded specimens was measured by Vickers micro-hardness tester with an indenter load of 10 N and an indentation time of 20 s (Arulmurugan *et al*., 2020, 2021c). Figure 2 shows a photograph of hardness specimen cut from the welded plate.

Figure 2. Mechanical test specimen

3. Results and Discussion

3.1 Tensile test

Following ASTM E08 standards, tensile strengths of the welded specimens were measured. The experimental design is shown in Table 3. Figure 3 (a) depicts the variation of tensile strength with respect to the considered process parameters. The welding speed of 30 mm/min shows a good tensile strength of welded parts. It was also noted that there was an increase in tensile strength due to the uniform distribution of temperature in the weld region when the rotational speed of weld tool was increased. However, increasing the rotational speed beyond 1500 rpm caused distortion at the welded region with an adverse effect. The tensile strength of 117 MPa in the Trial 4 shows a good result with rotational speed of 1300rpm, welding speed of 30mm/min and the axial load of 9kN. Figures 3 b, c and d depict the relationships of tensile strength with rotational speed, welding speed and axial load, individually. It could be observed from Figures 4a and 4c that the tensile strength first increased and then decreased with rotational speed and axial load: it reached the maximum at level 2. In contrast, the tensile strength initially decreased and then increased with the welding speed, and the maximum value of tensile strength was found for the minimum welding speed, as shown in Figure 4b.

3.2 Micro-hardness Test

Figure 4 (a) shows the measured micro-hardness values of the specimens. The values were separately taken for the base material area and for the welded area, and are listed in Table 3. The results show that increasing welding speed above 30 mm/min with a rotational speed of 1500 rpm decreased the hardness. Hence the welding speed is critical above 30 mm/min, with the hardness 180HV for the specimen. The hardness of AA3103 and the hardness of welded area obtained were similar in trial 3, independent of welding speed, rotation and axial load.

Figures 4 b, c & d show the variation of micro-hardness against the manipulated process parameters individually. From Figure 4a it could be seen that the hardness was higher at the weld area, and at all regions the hardness was higher at 1500 rpm. From 4 (b), it could be seen that the hardness was higher at 30 mm/min welding speed and the values initially decreased and then increased with welding speed. Similarly, Figure 4 (c) depicts the trend of hardness increasing until 9 kN load, where it attained its highest value and then decreased. Overall, from Figures 4 a, b & c, it could be seen that the maximum hardness was achieved in the weld area, while the lowest hardness was in the AA3103 zone. From this it can be stated that the weldment had a higher strength than the base metal zone.

Table 3. FSW process parameters and mechanical test results

Trial no.	Rotational speed (rpm)	Welding speed (mm/min)	Axial load (kN)	Tensile strength (N/mm^2)	Microhardness (HV)		
					AA3103 zone	Weld zone	AA6063 zone
1	1000	30	11	75	126	153	54
2	1000	40	9	77	64	171	57
3	1000	50	7	88	63	163	65
4	1300	30	9	117	126	180	63
5	1300	40	7	106	64	163	44
6	1300	50	11	100	71	171	55
7	1500	30	7	98	126	176	63
8	1500	40	11	89	90	160	56
9	1500	50	9	86	123	152	60

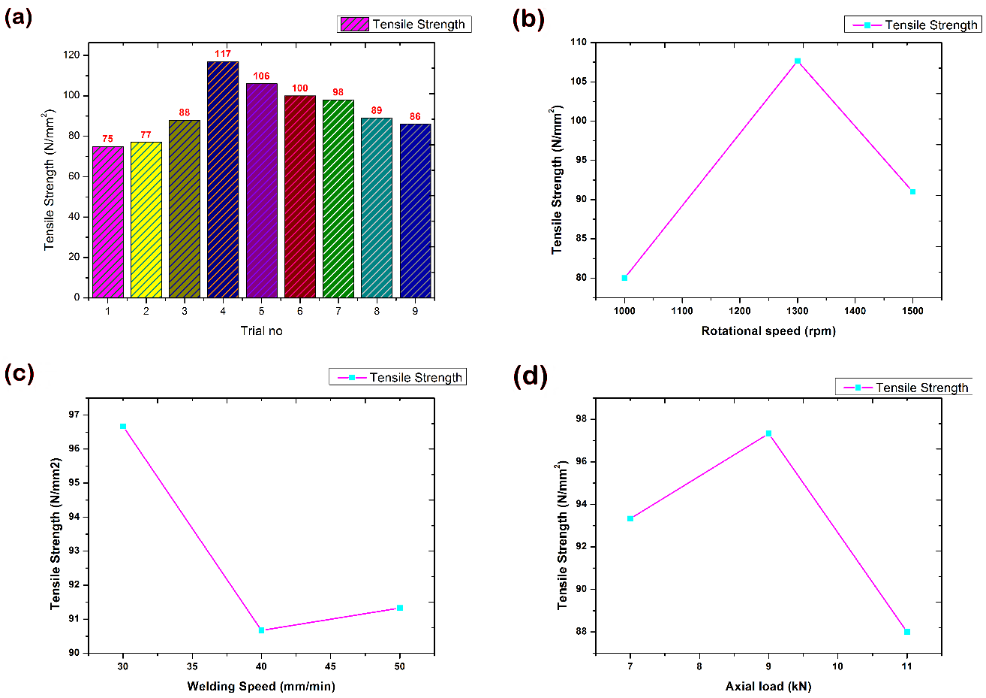

Figure 3. Variation of tensile strength with (a) process parameters, (b) rotational speed, (c) welding speed, and (d) axial load

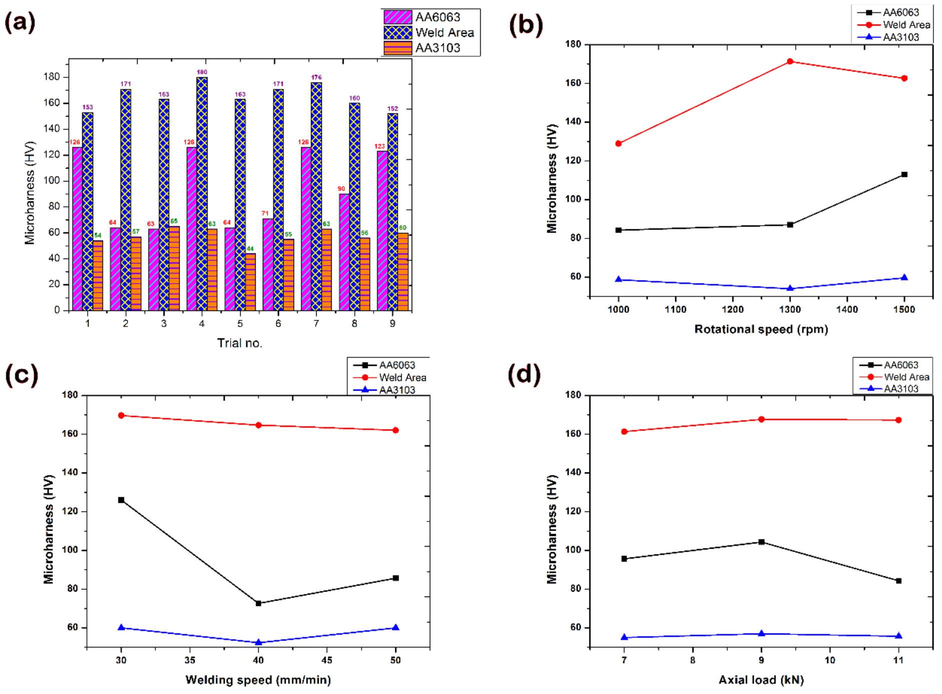

Figure 4. Variation of micro-hardness in different specimen zones

In order to visualize the temperature distribution during the FSW process, the weld plates were subjected to temperature analysis using ANSYS 15.0 software. Figure 5(a) shows the experimental conditions given as input to the ANSYS software, while 5(b) depicts the temperature distribution during the FSW process. From the figure, it could be noted that at the contact of tool and the workpiece, the temperature was at its maximum. HAZ could also be seen in the figure and it runs on both the sides of the weld along the path that the tool travels. Even during the welding of dissimilar metals, the HAZ was noted to be symmetrical about the weld line, which relates to the process homogeneity.

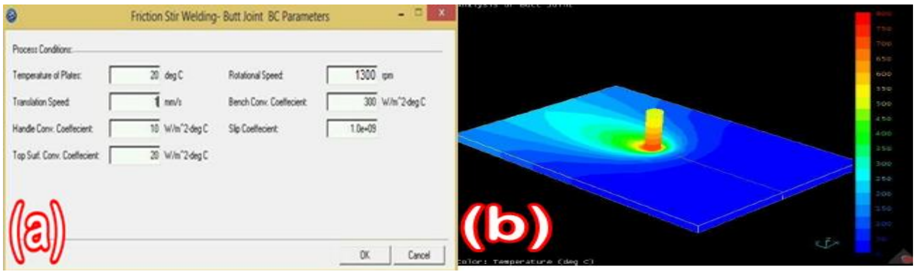

Figure 5. (a) Parameters of the FSW, and (b) ANSYS image of welded AA3130 & AA 6063

4. Conclusions

Aluminium alloys AA6063 and AA3103 as dissimilar alloy plates were welded using friction stir welding, and the mechanical properties of the weld plates were assessed. The experimental study supported the following conclusions:

- Tensile test results showed that a maximum tensile strength of 117 N/mm^2 was obtained when the rotational speed was kept as 1300 rpm, welding speed as 30 mm/min, and an axial load at 9 kN. Variations of tensile strength with the manipulated process parameters indicated that all of them had nonlinear effects without a consistent trend.
- Hardness results showed the maximum hardness of 126 HV at AA6063 region, 180 HV at the weld region, and 63 HV at AA3103 region for the operating conditions given above. The weld region had the maximum hardness larger than in the base metal region, due to the good compatibility of the tool with the weld specimens.
- ANSYS analysis portrayed a homogenous distribution of temperatures along the weld line, and the heat affected zone was visualized from the analysis. Overall, it could be stated that the 1300 rpm rotational speed, 30 mm/min welding speed, and 9 kN applied load gave a high mechanical strength weldment. Such friction stir welded parts find applications in electronic equipment, machine construction, and pressure vessels for cryogenic applications, where the use of aluminium alloys is inevitable.

References

Amirthagadeswaran, K. S. (2019). Corrosion and wear behaviour of nano Al2O3 reinforced copper metal matrix composites synthesized by high energy ball milling. *Particulate Science and Technology, 38*(2), 228-235.

Anbuchezhian, N., Devarajan, B., Priya, A. K., & Rajeshkumar, L. (2020). Machine learning frameworks for additive manufacturing–A review. *Solid State Technology, 63*(6), 12310-12319.

Arulmurugan, B., & Manikandan, M. (2018). Improvement of metallurgical and mechanical properties of gas tungsten arc weldments of Alloy 686 by current pulsing. *Transactions of the Indian Institute of Metals, 71*(12), 2953-2970.

Arulmurugan, B., Balaji, D., Rajkumar, S., Kamaraj, M., Mageshwaran, V., Sathishkumar, M., & Arivazhagan, N. (2021a). Influence of filler wire and welding process to mitigate the micro segregation of alloy C-2000 using continuous and pulsed current gas tungsten arc welding techniques. *Journal of Materials Engineering and Performance*, 1-18. doi:10.1007/s11665-021-05810-4.

Arulmurugan, B., Kumar, M. S., Balaji, D., Sathish, S., Rajkumar, S., Arivazhagan, N., & Manikandan, M. (2020). *Investigation on the effect of pulsed frequency on microstructure and hardness of alloy C-2000 by current pulsing* (No. 2020-28-0420). SAE Technical Paper.

Arulmurugan, B., Kumar, M. S., Kannan, T., Karuppiah, S., Kumaraguru, N., Ponsundar, E., & Manikandan, M. (2021c). Investigation on mechanical and microstructure characteristics of nickel based C-2000 super alloy using laser beam welding. *Materials Today: Proceedings, 43*, 3044-3049.

Arulmurugan, B., Modi, K., Sanjay, A. P., Yashwant, P. A., Rickwith, N., Mohan, C. G., & Arivazhagan, N. (2019). Effect of post-weld heat treatment on the microstructure and tensile properties of electron-beam-welded 21st century nickel-based super alloy 686. *Sādhanā, 44*(2), 38.

Arulmurugan, B., Sathishkumar, M., Balaji, D., Muralikrishnan, K., Pranesh, S., Praveen, V., & Manikandan, M. (2021b). Development of arc welding technique to preclude microsegregation in the dissimilar joint of alloy C-2000 and C-276. *Proceedings of the Institution of Mechanical Engineers, Part E: Journal of Process Mechanical Engineering*, 09544089211000011.

Bhuvaneswari, V., Priyadharshini, M., Deepa, C., Balaji, D., Rajeshkumar, L., & Ramesh, M. (2021). Deep learning for material synthesis and manufacturing systems: A review. *Materials Today: Proceedings*. doi:10.1016/j.matpr.2020.11.351.

Dietrich D., Nickel D., Krause M., 2011, Formation of intermetallic phases in diffusion welded joints of aluminium and magnesium alloys. *Journal of Materials Science 46*, 357-364.

Ganesan, M. C., Balasubramanian, A., Pasupathi, S., Mathiyazhagan, S., Govindasamy, R., Natarajan, A., & Manoharan, M. (2021). Influence of overalloyed filler wire to preclude the microsegregation in weld joint of alloy C-276. *Journal of Chemical Technology and Metallurgy, 56*(4), 853-856.

Genevois, C., Deschamps, A., Denquin, A., & Doisneau-Cottignies, B. (2005). Quantitative investigation of precipitation and mechanical behaviour for AA2024 friction stir welds. *Acta Materialia, 53*(8), 2447-2458.

John, A., Johny, K. J., Arulmurugan, B., Rajkumar, S., Arivazhagan, N., Naiju, C. D., & Manikandan, M. (2019). *Investigation on microstructure and mechanical properties of corrosion resistance alloy C-2000 fabricated by conventional arc welding technique* (No. 2019-28-0177). SAE Technical Paper.

Manikandan, M., Arivarasu, M., Arivazhagan, N., Puneeth, T., Sivakumar, N., Murugan, B. A., & Sivalingam, S. (2016). High temperature corrosion studies on pulsed current gas tungsten arc welded alloy C-276 in molten salt environment. *IOP Conference Series: Materials Science and Engineering* (Vol. 149, No. 1, p. 012020). doi:10.1088/1757899X/149/1/012020

Manikandan, M., Arivazhagan, N., Arivarasu, M., Mageshkumar, K., Rajan, D. N., Murugan, B. A., & Vimalanathan, R. (2017). Analysis of metallurgical and mechanical properties of continuous and pulsed current gas tungsten arc welded alloy C-276 with duplex stainless steel. *Transactions of the Indian Institute of Metals, 70*(3), 661-669.

Mao, Y., Ke, L., Liu, F., Huang, C., Chen, Y., & Liu, Q. (2015). Effect of welding parameters on microstructure and mechanical properties of friction stir welded joints of 2060 aluminum lithium alloy. *The International Journal of Advanced Manufacturing Technology, 81*(5), 1419-1431.

McLean, A. A., Powell, G. L. F., Brown, I. H., & Linton, V. M. (2003). Friction stir welding of magnesium alloy AZ31B to aluminium alloy 5083. *Science and Technology of Welding and Joining, 8*(6), 462-464.

Mishra, R. S., & Ma, Z. Y. (2005). Friction stir welding and processing. *Materials Science and Engineering: R: Reports, 50*(1-2), 1-78.

Mofid, M. A., Abdollah-Zadeh, A., & Ghaini, F. M. (2012). The effects of water cooling during dissimilar friction stir welding of Al alloy to Mg alloy. *Materials and Design* (1980-2015), 36, 161-167.

Nandan, R., DebRoy, T., & Bhadeshia, H. K. D. H. (2008). Recent advances in friction-stir welding–process, weldment structure and properties. *Progress in Materials Science, 53*(6), 980-1023.

Rajesh Kumar, L., Saravanakumar, A., Bhuvaneswari, V., Jithin Karunan, M. P., Raja, N. K., & Karthi, P. (2020a, February). Tribological behaviour of AA2219/MOS2 metal matrix composites under lubrication. *AIP Conference Proceedings* (Vol. 2207, No. 1, p. 020005).

Rajeshkumar, L. R. K. (2018). Dry sliding wear behavior of AA2219 reinforced with magnesium oxide and graphite hybrid metal matrix composites. *International Journal of Engineering Research and Technology, 6*, 3-8.

Rajeshkumar, L., Amirthagadeswaran, K. S., (2019). Variations in the properties of copper-alumina nanocomposites synthesized by mechanical alloying. *Materali in Technologije, 59*(1), 57–63. doi:10.17222/mit.2018.122

Rajeshkumar, L., Bhuvaneswari, V., Pradeepraj, B., & Palanivel, C. (2020b, October). Design and optimization of static characteristics for a steering system in an ATV. *IOP Conference Series: Materials Science and Engineering* (Vol. 954, No. 1, p. 012009).

Rajeshkumar, L., Suriyanarayanan, R., Hari, K. S., Babu, S. V., Bhuvaneswari, V., & Karunan, M. J. (2020b). Influence of boron carbide addition on particle size of copper zinc alloys synthesized by powder metallurgy. *IOP Conference Series: Materials Science and Engineering* (Vol. 954, No. 1, p. 012008).

Rajeshkumara, L., & Balajia, D. (2020). Study of mechanical and tribological properties of bio-ceramics reinforced aluminium alloy composites. *Solid State Technology, 63*(5), 4552-4560.

Rajkumar, S., Arulmurugan, B., Teklemariam, A., Tafesse, D., Mekonnen, A., Mulugeta. L., (2021a). Taguchi optimization of drilling process parameters on LM13/10 wt% Graphene composites made by stir casting process. *Materials Today: Proceedings*. doi:10.1016/j.matpr.2021.04.603

Rajkumar, S., Arulmurugan, B., Manikandan, M., Karthick, R., & Kaviprasath, S. (2017). Analysis of physical and mechanical properties of A3003 aluminum honeycomb core sandwich panels. *Applied Mechanics and Materials* (Vol. 867, pp. 245-253). Trans Tech Publications Ltd.

Rajkumar, S., Arulmurgan, B., & Muthuraman, S. (2018). Experimental and finite-element analysis of Tee joint's stiffness characteristics of a3003 honeycomb core sandwich panels. *International Journal of Mechanics and Design, 4*(2), 21-29.

Rajkumar, S., Arulmurugan, B., Teklemariam, A., Tafesse, D., Mekonnen, A., Mulugeta. L., (2021b). Investigation on mechanical properties of AA2024/HBN composites prepared by stir casting method. *Materials Today: Proceedings*. doi:10. 1016/j.matpr.2021.04.593,

Ramesh, M., Marimuthu, K., Karuppusamy, P., & Rajeshkumar, L. (2021). Microstructure and properties of YSZ-Al2O3 functional ceramic thermal barrier coatings for military applications. *Boletín de la Sociedad Española de Cerámica y Vidrio*. doi:10.1016/j.bsecv.2021.06.004

Rui-Dong, F., Zeng-Qiang, S., Rui-Cheng, S., Ying, L., Hui-jie, L., & Lei, L. (2011). Improvement of weld temperature distribution and mechanical properties of 7050 aluminum alloy butt joints by submerged friction stir welding. *Materials and Design, 32*(10), 4825-4831.

Saravanakumar, A., Bhuvaneswari, V., & Gokul, G. (2020a). Optimization of wear behaviour for AA2219-MoS2 metal matrix composites in dry and lubricated condition. *Materials Today: Proceedings, 27*, 2645-2649.

Saravanakumar, A., Rajeshkumar, L., Balaji, D., & Karunan, M. J. (2020b). Prediction of wear characteristics of AA2219-Gr matrix composites using GRNN and Taguchi-based approach. *Arabian Journal for*

Science and Engineering, 45(11), 9549-9557.

Saravanakumar, A., Saravanakumar, R., Sivalingam, S., & Bhuvaneswari, V. (2018b). Prediction capabilities of mathematical models for wear behaviour of AA2219/MgO/Gr hybrid metal matrix composites. *International Journal of Mechanical and Production Engineering Research and Development, 8*(8), 393-399.

Saravanakumar, A., Sivalingam, S., & Rajeshkumar, L. (2018a). Dry sliding wear of AA2219/Gr metal matrix composites. *Materials Today: Proceedings, 5*(2), 8321-8327.

Scialpi, A., De Filippis, L. A. C., & Cavaliere, P. (2007). Influence of shoulder geometry on microstructure and mechanical properties of friction stir welded 6082 aluminium alloy. *Materials and Design, 28*(4), 1124-1129.

Singh, G., Singh, K., & Singh, J. (2011). Effect of process parameters on microstructure and mechanical properties in friction stir welding of aluminum alloy. *Transactions of the Indian Institute of Metals, 64*(4), 325-330.

Upadhyay, P., & Reynolds, A. P. (2010). Effects of thermal boundary conditions in friction stir welded AA7050-T7 sheets. *Materials Science and Engineering: A, 527*(6), 1537-1543.

Xu, W., Liu, J., Luan, G., & Dong, C. (2009). Temperature evolution, microstructure and mechanical properties of friction stir welded thick 2219-O aluminum alloy joints. *Materials and Design, 30*(6), 1886-1893.

Zettler, R., Da Silva, A. A. M., Rodrigues, S., Blanco, A., & dos Santos, J. F. (2006). Dissimilar Al to Mg alloy friction stir welds. *Advanced Engineering Materials, 8*(5), 415-421.

Zhang, F., Su, X., Chen, Z., & Nie, Z. (2015). Effect of welding parameters on microstructure and mechanical properties of friction stir welded joints of a super high strength Al–Zn–Mg–Cu aluminum alloy. *Materials and Design, 67*, 483-491.